The 2009 IEEE/RSJ International Conference on
Intelligent Robots and Systems
October 11-15, 2009 St. Louis, USA

Apply Nonlinear Filter ESDS to Quantized Sensor Data

Takanori Emaru, Ryou Sase, Yohei Hoshino and Yukinori Kobayashi

***Abstract*— Proportional-Integral-Derivative (PID) control is widely used to control mechanical systems. In PID control technique, however, there are limits to the accuracy of the resulting movement because of the influence of gravity, friction, and interaction of joints caused by modeling errors. Digital acceleration control has robustness for the modeling errors. But it requires position, velocity, and acceleration of a controlled object to construct a controller. In this paper, we use the novel digital differentiator, ESDS. It enables digital acceleration control without increasing the number of sensors. Furthermore, the proposed method works effectively for quantized sensor data. The validity of the proposed method is confirmed by simulations and experiments using 2-link manipulator.**

I. INTRODUCTION

Mechanical systems generally employ PID control to control objects like robot manipulators. However, there are limits to the control accuracy because of modeling errors, which are caused by the influence of gravity, friction, and the interaction of joints. Here, digital acceleration control[1] is more robust towards modeling errors, and it is more effective control method than PID control.

Digital acceleration control requires accurate information of the position, velocity and acceleration. Accordingly, a digital acceleration controller must be equipped with sensors, while at the same time it is desirable to minimize the number of sensors used, to reduce the cost and maintenance. Estimates of velocity and acceleration from some position reduce employing additional sensors.

In order to construct a controller without increasing the number of sensors, we estimate velocity and accelerated velocity from position by using some differentiator. Generally, a motor is used as a actuator of mechanical systems. In order to obtain information of motor's angle, rotary encoder is commonly used. However, it is impossible to infinitely diminish a resolution of encoder. This causes a problem of quantization error. Especially, when a sampling time of control system becomes shorter by introducing a digital signal processor, cancellation of significant digits tends to increase. By using differential data that is affected by quantized error, then stability of the control system may become impaired. In position servo system, the encoder information becomes nondense when the velocity is near to zero. Therefore, it is impossible to perform high-precision position control.

In order to solve such problems, instantaneous speed observer is proposed[2][3]. The basic idea of this method is to lengthen a sampling time of encoder. As a result, adverse affect of cancellation of significant digits becomes small. However, when the amplitude of desired value is very minute, the adverse affect of nonlinear term such as static friction becomes large. In order to prevent the problem, a disturbance compensator is required, but system becomes complex. Furthermore, the same problem will occur when the targeted velocity is small.

In this paper, we use ESDS[4] as a differentiator. ESDS is one of the nonlinear filters that is based on sliding mode technique. It works very effectively to eliminate the impulse noise by preserving the sudden shift of input signals. In this paper, we improve ESDS with considering the quantized error of input signal. We propose a novel controller of digital acceleration control which includes ESDS as differentiator. We apply the proposed control system to 2-link manipulator, and we confirm the validity of the proposed method by performing simulations and experiments.

T. Emaru is with Graduate School of Engineering, Hokkaido University, N13W8, Sapporo, 060-8628, Japan emaru@eng.hokudai.ac.jp

II. DIGITAL ACCELERATION CONTROL

Controlling of the mechanical systems are affected by modeling errors. Modeling errors cause reductions in accuracy. Digital acceleration control [1], however, is robust to modeling errors, and this paper employs digital acceleration control.

The relation between input τ and time t is shown in Fig. 1. Here T is the control period. The equations of motion of a manipulator are expressed as:

$$\boldsymbol{\tau}(kT^+) = \boldsymbol{M}[\boldsymbol{\theta}(kT^+)]\ddot{\boldsymbol{\theta}}(kT^+) + \boldsymbol{X}[\boldsymbol{\theta}(kT^+), \dot{\boldsymbol{\theta}}(kT^+)], \tag{1}$$

$$\boldsymbol{\tau}(kT^-) = \boldsymbol{M}[\boldsymbol{\theta}(kT^-)]\ddot{\boldsymbol{\theta}}(kT^-) + \boldsymbol{X}[\boldsymbol{\theta}(kT^-), \dot{\boldsymbol{\theta}}(kT^-)]. \tag{2}$$

Equation (1) is the equation of motion at the time $t = kT^+$ when the input torque is applied, and Equation (2) is the equation of motion at the time $t = kT^-$, the moment immediately before $t = kT^+$.

Using the terms for the coriolis and centrifugal force $\boldsymbol{h}$, viscous friction $\boldsymbol{D}$, coulomb and static friction $\boldsymbol{E}$, and gravity $\boldsymbol{g}$, the term $\boldsymbol{X}$ is described by

$$\boldsymbol{X}[\boldsymbol{\theta}, \dot{\boldsymbol{\theta}}] = \boldsymbol{h}[\boldsymbol{\theta}, \dot{\boldsymbol{\theta}}] + \boldsymbol{D}\dot{\boldsymbol{\theta}} + \boldsymbol{E}[\boldsymbol{\theta}, \dot{\boldsymbol{\theta}}] + \boldsymbol{g}[\boldsymbol{\theta}]. \tag{3}$$

Although $\boldsymbol{\tau}$ and $\ddot{\boldsymbol{\theta}}$ is renewed at $t = kT^+$, $\boldsymbol{\theta}$ and $\dot{\boldsymbol{\theta}}$ are not, because they are integrals of the acceleration. This leads to the following relations:

$$\boldsymbol{\theta}(kT^+) = \boldsymbol{\theta}(kT^-), \tag{4}$$

$$\dot{\boldsymbol{\theta}}(kT^+) = \dot{\boldsymbol{\theta}}(kT^-). \tag{5}$$

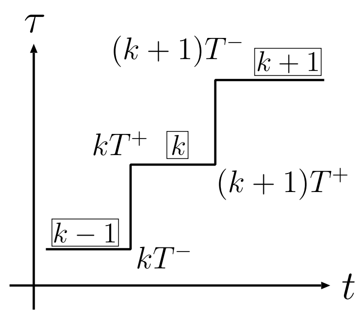

Fig. 1. Relation between input (τ) and time (t)

Subtracting Eq. (2) from Eq. (1) and using Eqs. (4) and (5) give

$$\boldsymbol{\tau}(kT^+) = \boldsymbol{\tau}(kT^-) + \boldsymbol{M}[\boldsymbol{\theta}(kT^+)] \{\ddot{\boldsymbol{\theta}}(kT^+) - \ddot{\boldsymbol{\theta}}(kT^-)\}. \quad (6)$$

This equation represents the advantage of digital acceleration control. Because the $\boldsymbol{X}$ term which causes modeling errors is not included in Eq. (6), modeling errors do not affect the accuracy. In Eq. (6) $\ddot{\theta}(kT^+)$ is assigned as the desired acceleration $\ddot{\theta}_d(kT^+)$, and adding PD compensation to acceleration, with Eqs. (4) and (5), the following equation is obtained:

$$\begin{aligned}\boldsymbol{\tau}(kT^+) &= \boldsymbol{\tau}(kT^-) + \boldsymbol{M}[\boldsymbol{\theta}(kT^+)] \\ &\{\ddot{\boldsymbol{\theta}}_d(kT^+) - \ddot{\boldsymbol{\theta}}(kT^-) + \boldsymbol{K}_D[\dot{\boldsymbol{\theta}}_d(kT^+) \\ &- \dot{\boldsymbol{\theta}}(kT^+)] + \boldsymbol{K}_P[\boldsymbol{\theta}_d(kT^+) - \boldsymbol{\theta}(kT^+)]\}.\end{aligned} \quad (7)$$

This equation determines the input torque of the digital acceleration control.

Now, the stability of digital acceleration control will be discussed. The angular error is defined as

$$\boldsymbol{e}(t) = \boldsymbol{\theta}_d(t) - \boldsymbol{\theta}(t), \quad (8)$$

where $\boldsymbol{\theta}_d$ is the desired angle, and with Eqs. (6), (7), and (8), the following is derived:

$$\ddot{\boldsymbol{e}}(kT^+) + \boldsymbol{K}_D\,\dot{\boldsymbol{e}}(kT^+) + \boldsymbol{K}_P\,\boldsymbol{e}(kT^+) = 0. \quad (9)$$

In the very short time interval $[kT^+\ (k{+}1)T^+]$, the following approximation is made:

$$\dot{\boldsymbol{e}}((k+1)T^+) \simeq \dot{\boldsymbol{e}}(kT^+) + \ddot{\boldsymbol{e}}(kT^+)T, \quad (10)$$

$$\boldsymbol{e}((k+1)T^+) \simeq \boldsymbol{e}(kT^+) + \dot{\boldsymbol{e}}(kT^+)T + \ddot{\boldsymbol{e}}(kT^+)\tfrac{T^2}{2}. \quad (11)$$

Using Eq. (9) and eliminating $\ddot{\boldsymbol{e}}(kT^+)$ in Eqs. (10) and (11), they can be rewritten in matrix form as

$$\begin{bmatrix}\boldsymbol{e}((k+1)T^+)\\ \dot{\boldsymbol{e}}((k+1)T^+)\end{bmatrix} = \begin{bmatrix}\boldsymbol{I} - \frac{T^2}{2}\boldsymbol{K}_P & T\boldsymbol{I} - \frac{T^2}{2}\boldsymbol{K}_D \\ -T\boldsymbol{K}_P & \boldsymbol{I} - T\boldsymbol{K}_D\end{bmatrix}\begin{bmatrix}\boldsymbol{e}(kT^+)\\ \dot{\boldsymbol{e}}(kT^+)\end{bmatrix}, \quad (12)$$

$$\boldsymbol{E}(k+1^+) = \boldsymbol{A}\boldsymbol{E}(k^+). \quad (13)$$

When the coefficient matrixes $\boldsymbol{K}_P$ and $\boldsymbol{K}_D$ are selected as the system is stable, the errors converge to zero. However, it is difficult to determine $\boldsymbol{K}_P$ and $\boldsymbol{K}_D$ by trial and error as the system is stable and has a high tracking capability. Developing $\boldsymbol{A}$ in Eq. (13), we find

$$\begin{aligned}&\begin{bmatrix}\boldsymbol{I} - \frac{T^2}{2}\boldsymbol{K}_P & T\boldsymbol{I} - \frac{T^2}{2}\boldsymbol{K}_D \\ -T\boldsymbol{K}_P & \boldsymbol{I} - T\boldsymbol{K}_D\end{bmatrix} \\ &= \begin{bmatrix}\boldsymbol{I} & T\boldsymbol{I}\\ \boldsymbol{0} & \boldsymbol{I}\end{bmatrix} - \begin{bmatrix}\frac{T^2}{2}\boldsymbol{I}\\ T\boldsymbol{I}\end{bmatrix}\begin{bmatrix}\boldsymbol{K}_P & \boldsymbol{K}_D\end{bmatrix} \\ &= \boldsymbol{A}_1 - \boldsymbol{A}_2\boldsymbol{K},\end{aligned} \quad (14)$$

and Eq. (13) can be represented as

$$\boldsymbol{E}(k+1^+) = (\boldsymbol{A}_1 - \boldsymbol{A}_2\boldsymbol{K})\boldsymbol{E}(k^+). \quad (15)$$

Now Eq. (15) is in a form for state feedback control, and $\boldsymbol{K}_P$ and $\boldsymbol{K}_D$ can be determined by pole assignment or optimal regulator theory. Therefore the selection of parameters for the digital acceleration control is simpler than with PID control.

III. ESDS

Digital acceleration control is an effective control method, however, additional sensors to measure velocity and acceleration are needed. Therefore, a system that Estimates the Smoothed and Differential values by a Sliding mode (ESDS) [4] [5] is employed to estimate velocity and acceleration from rotational angle. In this section, the theorem for system configuration and the actual implementations by using the two kinds of stable systems are described. The composition of our estimator is as follows:

$$\begin{cases}\dot{x_1} = x_2\\ \dot{x_2} = f(x_1, x_2, y)\end{cases} \quad (16)$$

Our proposed system is shown in Fig. 2. In this system, the input signal y contains the target element of signal $\hat{y}$ and the noisy element of signal n. If the parameter x_1 ignores the noisy element n and follows the target element $\hat{y}$, we obtain the desirable smoothed value. Furthermore, the relation $\dot{x_1} = x_2$ in (16) shows that the parameter x_2 is the estimated differential of $\hat{y}$.

Theorem 1: If the following system

$$\begin{cases}\dot{x_1} = x_2\\ \dot{x_2} = f(x_1, x_2)\end{cases} \quad (17)$$

is globally uniform and asymptotically stable at the origin,

$$\begin{cases}\dot{x_1} = x_2\\ \dot{x_2} = R^2 f(x_1 - y, x_2/R)\end{cases} \quad (18)$$

Then the status $x_1(t)$ of these differential equations conform to constant signal $y(t) = C$ in the finite time for $R \gg 0$. Where R is an arbitrary parameter given by the system designer, and it dominates the characteristics of system convergence.

The proof of this theorem is see reference [6]. This theorem says that a globally uniform asymptotically stable system at the origin is required in order to construct the estimator. As a stable system, we consider the following two kinds of systems:

1) The sliding mode system that has linear switching line.
2) The sliding mode system that has nonlinear switching line. This system is generally known as the minimum-time system.

In this section, we construct two estimators by using these stable systems.

A. Utilize the Sliding Mode System that has Linear Switching Line

As described in Theorem 1, a globally uniform asymptotically stable system at the origin is required in order to construct the estimator. As the stable system, we utilize the sliding mode system that has linear switching line in this subsection. At the beginning, we explain the sliding mode system. We start with the consideration of system configuration on the basis of the following second-order dynamic system.

$$\begin{cases} \dot{x_1} = x_2 \\ \dot{x_2} = u \end{cases} \tag{19}$$

In (19), we find the input signal u that converges the arbitrary state variable (x_1, x_2) to the origin. By finding this u, we can obtain the system that is globally uniform and asymptotically stable at the origin. If we consider this system from a physical standpoint, it will be like accelerating an object moving in one-dimensional space then stopping it at the origin. In this case, there is a limit to the amplitude of the applied acceleration ($|u| \leq U, U > 0$). In order to analyze this system, we perform a phase plane analysis. Phase plane analysis [7] is a graphical method for investigating second-order systems. The basic idea of it is to generate, in the state space of a second-order dynamic system (a two-dimensional plane called the phase plane), motion trajectories corresponding to various initial conditions, and then to examine the qualitative features of the trajectories. In this way, information concerning the transient response of the system can be obtained.

From (19), we have

$$\begin{aligned} \dot{x_2} &= u \\ x_2\dot{x_2} &= ux_2 = u\dot{x_1} \\ \int x_2 dx_2 &= u\int dx_1 \\ x_2^2/2 &= ux_1 + c \end{aligned} \tag{20}$$

The phase planes of (20) when $u > 0$ and $u < 0$ are shown in Figs. 3(a) and (b). In order to obtain the stable system, we set the switching line at $x_2 = -ax_1 (a > 0)$, and apply the input of $u = -U$ when the state exists above the switching line and the input of $u = +U$ below the switching line. The solution trajectory in the phase plane is illustrated as

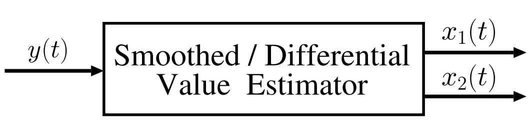

Fig. 2. View of estimator.

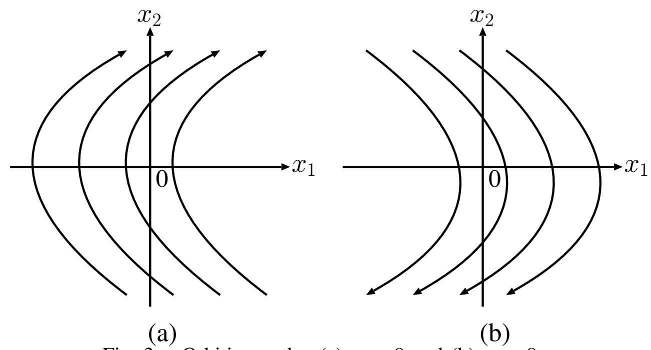

Fig. 3. Orbiting paths: (a) $u > 0$ and (b) $u < 0$.

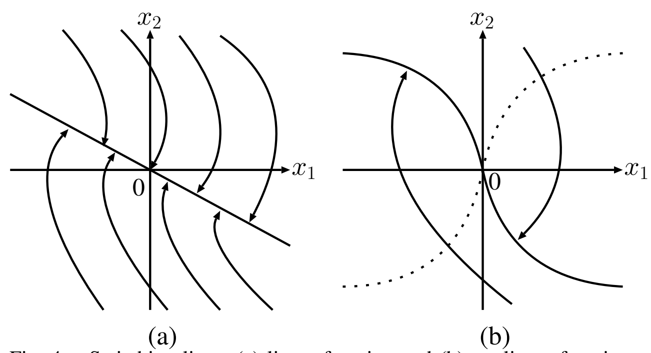

Fig. 4. Switching lines: (a) linear function and (b) nonlinear function.

shown in Fig. 4(a), and the state from the arbitrary initial condition converges to the origin according to the trajectory. This concept of system configuration is based on the sliding mode technique. In this way, we can obtain the stable system from the sliding mode theory. Fig. 4(a) is formulated by following differential equations.

$$\begin{cases} \dot{x_1} = x_2 \\ \dot{x_2} = -U\mathrm{sign}(x_2 + ax_1) \end{cases} \tag{21}$$

where the sign indicates the signum function and is defined by the following equation.

$$\mathrm{sign}(\sigma) = \begin{cases} +1 & \sigma > 0 \\ 0 & \sigma = 0 \\ -1 & \sigma < 0 \end{cases} \tag{22}$$

The system represented in (21) is globally uniform and asymptotically stable at the origin. Therefore, we can construct the following estimator by applying the Theorem 1.

$$\begin{cases} \dot{x_1} = x_2 \\ \dot{x_2} = -UR^2\mathrm{sign}(a(x_1 - y) + x_2/R) \end{cases} \tag{23}$$

When we apply ESDS to an actual system, chattering problem may occur. To reduce the chattering effect, saturation function is generally used in place of signum function as shown in next equations.

$$\begin{cases} \dot{x}_1 = x_2 \\ \dot{x}_2 = -UR^2\mathrm{sat}\,(\sigma/\phi) \end{cases} \tag{24}$$

$$\sigma = Sx_1 + x_2 \tag{25}$$

Where $aR = S$. We call it ESDS-linear. The definition of saturation function is as follows:

$$\text{sat}\left(\frac{\sigma}{\phi}\right) = \begin{cases} \sigma/\phi & (|\sigma| \le \phi) \\ \text{sign}(\sigma) & (|\sigma| \ge \phi) \end{cases} \tag{26}$$

The characteristics of ESDS-linear are described in next section.

B. Utilize the Sliding Mode System that has Nonlinear Switching Line

In previous subsection, we have constructed the estimator by using the sliding mode system that has linear switching line. According to the Theorem 1, the estimated smoothed and differential values are obtained when the estimate of the input signal coincides with the input signal. Therefore, it is expected that the estimation of the input signal is obtained rapidly if the system converges quickly. To this end, we find the switching line that converges the arbitrary initial states to the origin in minimum-time by using the Pontryagin's maximum principle [8]. The optimal switching line for $|u| \le U$ is illustrated in Fig. 4(b) and is formulated as follows:

$$\begin{cases} \dot{x_1} = x_2 \\ \dot{x_2} = -U\text{sign}(Ux_1 + x_2|x_2|/2) \end{cases} \tag{27}$$

These differential equations represent the optimal trajectory and they are generally known as the minimum-time system. Equation (27) indicates that the trajectory is a segment of the parabola. The system represented in (27) is globally uniform and asymptotically stable at the origin, and this system converges from arbitrary initial points to the origin in minimum-time under the condition of (19). We can construct the following estimator by using (27).

$$\begin{cases} \dot{x_1} = x_2 \\ \dot{x_2} = -UR^2\text{sign}(U(x_1 - y) + |x_2|x_2/(2R^2)) \end{cases} \tag{28}$$

As same as ESDS-linear, we introduce the saturation function to (28). As a result, next equations are obtained:

$$\begin{cases} \dot{x}_1 = x_2 \\ \dot{x}_2 = -UR^2\text{sat}\left(\frac{\sigma}{\phi}\right) \end{cases} \tag{29}$$

$$\sigma = 2UR^2(x_1 - y) + |x_2|x_2 \tag{30}$$

We call this system as ESDS-minimum.

In this section, two kinds of estimators are constructed by using the Theorem 1, and ESDS-linear and ESDS-minimum are obtained. In the following sections, we draw a comparison between them in order to clarify the characteristics of ESDS.

IV. Evaluation of the Proposed Differentiator

In order to perform the evaluation of the proposed ESDS, simulation results by using pendulum are shown in this section. In this simulation, we estimate the angular velocity and angular acceleration from angle. In order to evaluate the performance of the proposed methods, we draw a comparison between estimated value and true value that is calculated by using Runge-Kutta method. We use quantized input value in order to apply the proposed method to actual mechanical systems. The specification of the pendulum is shown in Table I.

TABLE I
Spec of Pendulum

length	l	0.4 m
acceleration of gravity	g	9.81 m/s^2
initial angle	θ_0	25 deg
initial angular velocity	ω_0	0 deg/s

TABLE II
Parameters of ESDS-linear

ESDS1		ESDS2	
UR_1^2	30	UR_2^2	30
S_1	30	S_2	25
ϕ_1	1	ϕ_2	4

TABLE III
Parameters of ESDS-minimum

ESDS1		ESDS2	
UR_1^2	30	UR_2^2	30
ϕ_1	1	ϕ_2	4

1) ESDS-linear: Table II shows the parameters of ESDS-linear, and Fig. 5 shows the simulation result. This simulation result shows that angular velocity and angular acceleration are accurately estimated by using ESDS-linear.

2) ESDS-minimum: Table III shows the parameters of ESDS-minimum, and Fig. 6 shows the simulation result. This simulation result shows that there is a little error especially on the estimated accelerated velocity.

Ideally, estimated value by using ESDS-minimum is considered more accurate than ESDS-linear because ESDS-minimum utilizes the minimum-time system. However, simulation results are different. Therefore, we discuss about the cause of this problem in the next section.

V. Improvement of ESDS

From the simulation results of the previous section, estimated accelerated velocity of ESDS-minimum is vibrated at velocity zero. In this section, we discuss the cause of the vibration, and we propose the novel ESDS which control the vibration.

In order to discuss about the cause of the vibration, we illustrate the switching line on phase plane as shown in Fig. 7. This figure shows that the gradient of switching line of the minimum-time system becomes infinity at the convergence point. Therefore, the influence of the error of the input signal to the differential value grows larger than linear system.

The simulation results, which were shown in the previous section, had been influenced by quantized data. In order to calculate accelerated velocity, we apply ESDS twice. At the first ESDS, estimated differential value is influenced by the quantized error especially at the convergence point. And then, the differential value that was influenced by quantized error is inputted to the second ESDS. As a result, the quantized error is amplified especially at the estimated accelerated velocity in the second ESDS. On the basis of this consideration, we improve the switching line of ESDS.

Basically, ESDS-minimum is superior to ESDS-linear in terms of convergence speed. On the other hand, ESDS-linear is superior to ESDS-minimum in terms of stability at the convergence point. In this way, there is a trade-off between these two conditions. Therefore, we improve the switching line of ESDS in order to satisfy these two conditions. At the

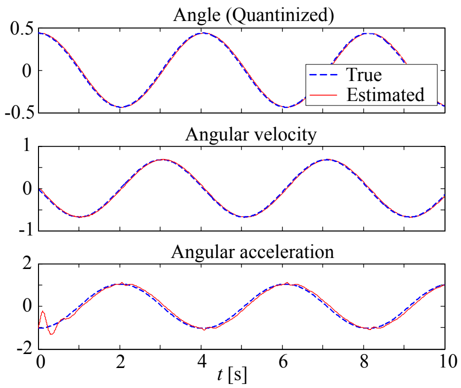

Fig. 5. Simulation of pendulum (ESDS-linear)

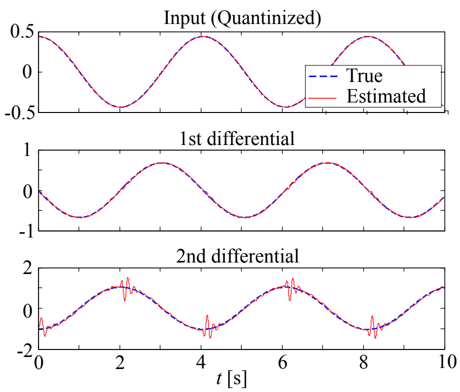

Fig. 6. Simulation of pendulum (ESDS-minimum)

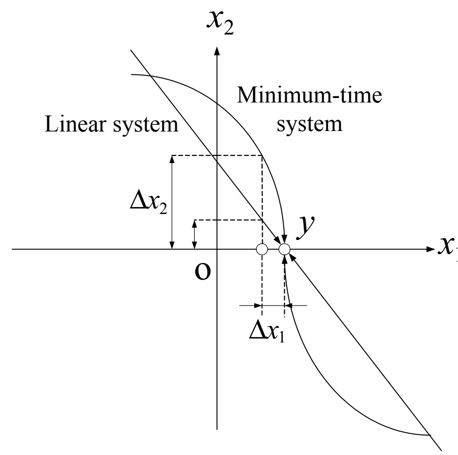

Fig. 7. Convergence point on phase plane

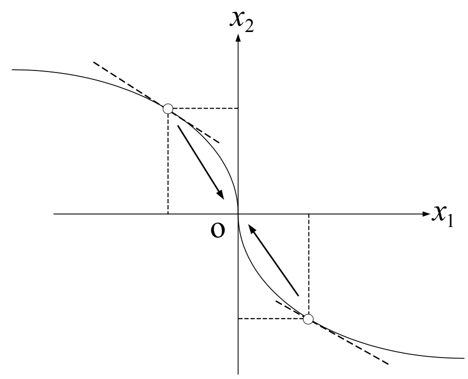

Fig. 8. Concept of modification

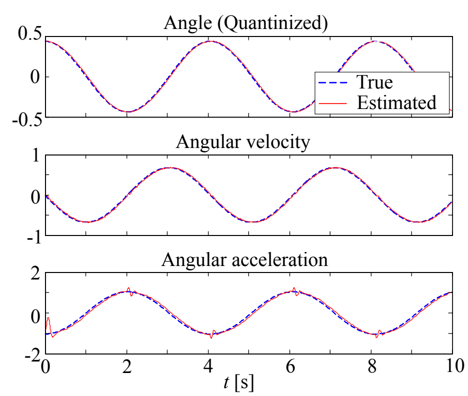

Fig. 9. Simulation of pendulum (ESDS-quantized)

beginning, we move the switching line of ESDS-minimum parallelly so that the gradient of the switching line at the convergence point becomes $-S'$. Namely, the following equation is satisfied:

$$\frac{dx_2}{dx_1} = -S' \tag{31}$$

Then, we move parallelly the switching line so that the following coordinates become origin.

$$(x_1, x_2) = \left(-\frac{U}{2S'^2}, \frac{U}{S'}\right), \left(\frac{U}{2S'^2}, -\frac{U}{S'}\right) \tag{32}$$

The switching line that satisfies above-mentioned is represented by following-equation:

$$\sigma = 2UR^2\left(x_1 - y\right) + |x_2|\, x_2 + \frac{2UR^2}{S} x_2 \tag{33}$$

Figure 9 shows the simulation result by using new-ESDS that utilizes the improved switching line. We define this ESDS as ESDS-quantized. From the next section, we use the ESDS-quantized as ESDS.

VI. Simulation

A. Modeling of a manipulator

This section models a horizontal planar 2-link manipulator as shown in Fig. 10, applying digital acceleration control to a horizontal planar 2-link manipulator. The specifications of the manipulator in the simulations and experiments are shown in Table IV.

In modeling the horizontal planar 2-link manipulator, the followings were assumed:

- The links are rigid.
- It is unable to ignore the effect of coriolis and centrifugal forces.
- Angles are quantized by the equation:

$$y = q \cdot \mathrm{round}(\theta/q), \tag{34}$$

where θ: input, y: output, q: resolution, and round: a rounding function.

The last of the assumptions is the most important in actual

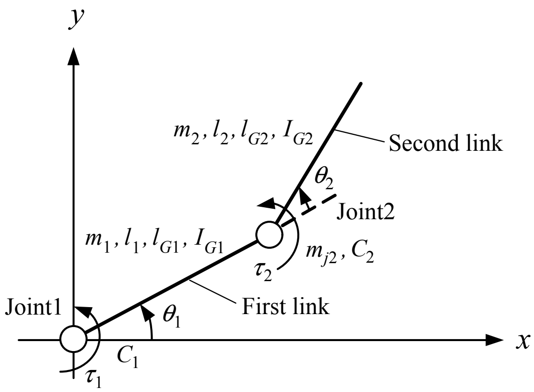

Fig. 10. Horizontal planar 2-link manipulator model

TABLE IV
SPECIFICATIONS OF THE MANIPULATOR

First link		Second link	
m_1	0.096 kg	m_2	0.096 kg
		m_{j2}	0.40 kg
l_1	0.12 m	l_2	0.12 m
l_{G1}	0.06 m	l_{G2}	0.06 m
I_{G1}	4.61×10^{-4} kg · m^2	I_{G2}	4.61×10^{-4} kg · m^2
C_1	1.0×10^{-4} Nm · s	C_2	1.0×10^{-4} Nm · s
q_1	$2\pi/4096$	q_2	$2\pi/4096$

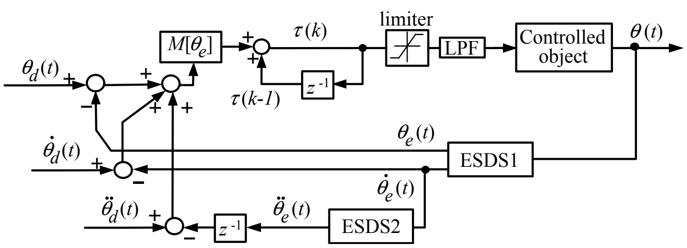

Fig. 11. Block diagram of the control system

equipment as sensors of actual equipment have limited resolution. The equation of motion is derived by using the Lagrangian method:

$$\begin{bmatrix} J_1 + J_2 + J_3 \cos\theta_2 & J_2 + \frac{1}{2}J_3\cos\theta_2 \\ J_2 + \frac{1}{2}J_3\cos\theta_2 & J_2 \end{bmatrix} \begin{pmatrix} \ddot{\theta}_1 \\ \ddot{\theta}_2 \end{pmatrix} + \begin{bmatrix} -J_3\dot{\theta}_1\dot{\theta}_2 \sin\theta_2 - \frac{1}{2}J_3\dot{\theta}_2^2\sin\theta_2 \\ \frac{1}{2}J_3\dot{\theta}_1^2 \sin\theta_2 \end{bmatrix} + \begin{bmatrix} \tau_{fric1} \\ \tau_{fric2} \end{bmatrix} = \begin{pmatrix} \tau_1 \\ \tau_2 \end{pmatrix}, \quad (35)$$

where J_1, J_2, J_3 are

$$J_1 = m_1 l_{G1}^2 + m_2 l_1^2 + m_{j2} l_1^2 + I_{G1}, \quad (36)$$

$$J_2 = m_2 l_{G2}^2 + I_{G2}, \quad (37)$$

$$J_3 = 2 m_2 l_1 l_{G2}. \quad (38)$$

B. Composition of the control system

Combining the ESDS with a digital acceleration control, the control system is composed as shown in Fig. 11. Because the ESDS does not estimate second order differential values, ESDS is employed twice to estimate angular acceleration.

TABLE V
PARAMETERS OF ESDS

ESDS1		ESDS2	
UR_1^2	1000	UR_2^2	3000
S_1	80	S_2	75
ϕ_1	50	ϕ_2	500

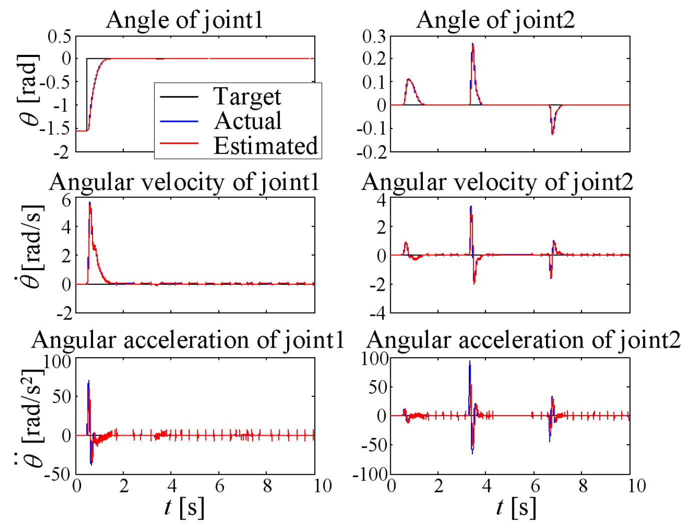

Fig. 12. Simulation results under payload changes

The torque of the controller must be restricted to improve the initial response, and a Low Pass Filter (LPF) is applied to the input torque to reduce high frequency components in the estimated acceleration. In both the simulations and experiments, the desired angles of joints θ_d are given by

$$\theta_d(t) = a \sin(t/b) \quad (39)$$

and the control period T is 2 ms. Parameters of the digital acceleration control are: $\boldsymbol{K}_p = \text{diag}(50, 80)$ and $\boldsymbol{K}_d = \text{diag}(12, 15)$. And parameters of ESDS-quantized are shown in Table V.

C. Simulation Results

Figure 12 shows the simulation results. In order to confirm the validity of the proposed system, we performed the simulation under payload changes. As the initial condition, the manipulator grasps a object that weight is 0.05 kg. At $t = 3.3$ s, the manipulator releases the object so payload becomes 0. And then, the manipulator grasps a same object when $t = 6.7$ s. Simulation results show that the disturbance to the controlled angle by using the proposed method is tiny in spite of the existence of payload changes. The robustness to payload changes is one of the advantages of digital acceleration control method.

VII. Experimental Results

We performed the experiments under same conditions as the simulations which were performed in the previous section. In order to realize the structure to change payload, the electromagnet is attached to the manipulator as shown in

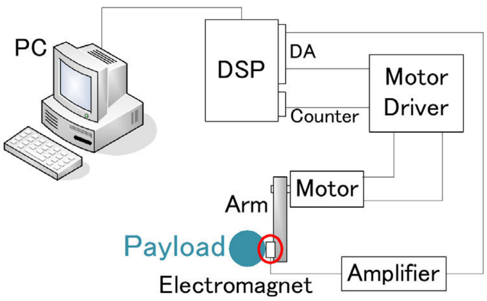

Fig. 13. Block diagram of the experimental setup

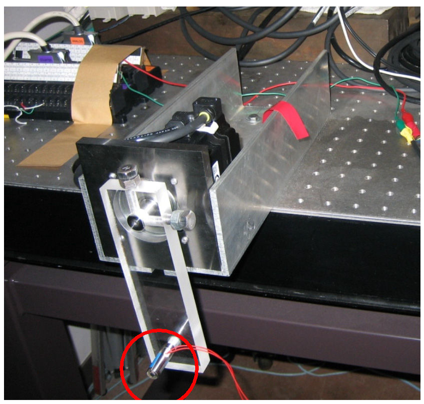

Fig. 14. Experimental setup

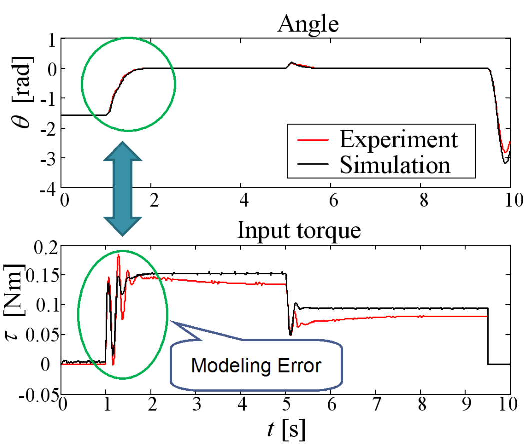

Fig. 15. Experimental results

Figs. 13 and 14. Therefore, it is easy to release a payload, but it is difficult to attach a payload on manipulator. So, we don't perform the experiment of grasping object. As the initial condition, the manipulator grasps an object of 0.05 kg. At $t = 5$ s, the manipulator releases the object, therefore payload becomes 0.

Figure 15 shows the experimental result. This result shows the validity of the proposed control system under payload changes. However, we can observe an adverse affect to the angle when payload changes. The cause of the adverse affect is delay of input signal because of using the LPF. And we can observe a little difference between simulation and experimental result on input torque. The causes of the difference are considered modeling error and static friction. It is possible that the coefficient of viscous damping of actual manipulator is different from the parameter of simulation. It is difficult to determine the accurate value because the value is affected by the environment and conditions used.

As mentioned above, there is a difference between simulation and experimental result on input torque. However, the error on input torque does not affect a controlled angle. This result shows the validity of the digital acceleration control method including ESDS-quantized. In other words, there is a strong consistency between simulation and experimental result. Therefore, by using the digital acceleration control method, the usefulness of the simulation improves.

VIII. CONCLUSIONS

Simulations and experiments were performed on digital acceleration control with the ESDS-quantized of a 2-link manipulator. We proposed the ESDS-quantized in order to differentiate quantized data such as angle that is obtained by encoder. It was shown that ESDS enables digital acceleration control without additional sensors. The results confirm the effectiveness and practicality of ESDS in actual machinery applications as well as in simulations. The ESDS employed in this paper requires LPF for estimates of acceleration of the control system, and further development of the ESDS is the subject for future study.

IX. ACKNOWLEDGMENTS

This work was supported by a research grant from The Mazda Foundation.

REFERENCES

[1] S.Y. Wang, K. Takahashi, Y. Hashimoto, K. Hori, T. Tsuchiya, and M. Nakatsuyama, "The Estimation Method Velocity and Acceleration Using Fuzzy Reasoning and its Application to Robot Manipulator Trajectory Control," *Fuzzy Theory and System*, vol. 8, no. 2, pp. 571-583, 1997.

[2] Y. Hori, "High performance control of servomotors with low precision shaft encoder using instantaneous speed observer and adaptive identification of inertia moment", *in IEEE Asia-Pacific Workshop on Advances in Motion Control*, 1993, pp. 7–12.

[3] K. Ohishi and Y. Nakamura, "Robust speed servo system for wide speed range based on instantaneous speed observer and disturbance observer", *in IEEE. IES. 4th International Workshop on Advanced Motion Control*, 1996, pp. 326–331.

[4] T. Emaru and T. Tsuchiya, "Research on Estimating Smoothed Value and Differential Value By Using Sliding Mode System," *IEEE Transactions on Robotics and Automation*, vol. 19, no. 3, pp. 391-402, 2003.

[5] T. Emaru and T. Tsuchiya, "Research on Parameter Determination for Smoothed and Differential Value Estimator," *IEICE Transactions*, vol. E86-A, no. 7, pp. 1732-1741, 2003.

[6] T. Emaru and T. Tsuchiya, "Research on estimating smoothed value and differential value by using sliding mode system," *IEEE Trans. Robot. Automat.*, vol. 19, no. 3, pp. 391–402, June 2003.

[7] J. Jacques, E. Slotine, and W. Li., *Applied Nonlinear Control*. New Jersey: Prentice Hall, 1991.

[8] A.P. Sage and C.C. White, *Optimum systems control (second edition)*. New Jersey: Prentice-Hall, 1977.

[9] J.G.F. Francis, The QR Transformation I, *Comput. J.*, vol. 4, 1961, pp 265-271.

[10] H. Kwakernaak and R. Sivan, *Modern Signals and Systems*, Prentice Hall, Englewood Cliffs, NJ; 1991.

[11] D. Boley and R. Maier, "A Parallel QR Algorithm for the Non-Symmetric Eigenvalue Algorithm", *in Third SIAM Conference on Applied Linear Algebra*, Madison, WI, 1988, pp. A20.